Chapter 5

Feature Registration

With features extracted from both a base and target surface, feature registration can be performed before elastic surface registration in an attempt to improve the registration result. The use of feature points in mesh deformation is discussed using radial basis function interpolation (RBF) in this chapter.

The registration of feature lines is implemented with the help of literature resources and applied as an adaptation of the elastic surface registration procedure previously implemented. Registering feature lines as a step before elastic surface registration is then applied and illustrated. In creating the symmetric smooth skull, this step greatly improves the final registered result.

It is then applied to the registration of the orthognathic skull geometry with less success. Here the vast difference in topology and non-corresponding features are seen to cause undesired results. This is due to the way in which the registration is performed. All nodes and all surfaces are used in the original elastic registration procedure. This presents a few issues where points or surfaces on the target geometry have no equivalent on the generic mesh for example.

Because of the difficulty in registering the generic shape to the orthognathic skull form, it is suggested that only user selected features be registered along with featureless surfaces. The feature areas associated with unregistered features are then classified as forbidden and ignored during elastic surface registration. The generic mesh is deformed using only the registration on allowable surfaces. This suggestion greatly reduces the amount of user interference required in registering these complex geometries, as will be seen in Chapter 6.

5.1 Feature Point Registration

Feature points are classically marked manually in the study of geometric morphology. The landmark positions in Figure 1.1 for example could be obtained by marking these points on a skull with a digital stylus. The digitised landmark coordinates of a statistical sample of skulls can then be used in a statistical analysis where certain shape characteristics and their relationships are investigated.

Landmark coordinates could also be obtained manually or automatically from digital surface representations. Matched points on a surface mesh could be marked and the difference and similarity between shapes could be studied in the same way.

In this subsection, a short overview of Radial Basis Function (RBF) interpolation is discussed with particular detail given to the Thin Plate Spline (TPS) basis function. RBFs and specifically the TPS is most commonly used in geometric morphology to graphically represent the deformation or difference between generic and target landmark coordinates within a statistical sample [42, 54]. Deforming a base mesh to a target configuration may also be done using radial basis function interpolation as it is inexpensive. This is because connectivity is not required in deforming a mesh.

Shape context feature points are also commonly used in registration and is briefly mentioned in Appendix C. This is an automatic method for finding correspondences between all the points in a shape or feature points extracted after applying differential geometry for example. These points are classified using histograms within a greater shape context.

5.1.1 Radial Basis Function Interpolation

Radial Basis Function Interpolation can be applied to scattered data. If a spatial distribution of points exist with displacements or field values known at a select few locations for example, an interpolated field can be approximated.

In [26], RBF interpolation is used to update the mesh used in a Fluid Structure Interaction (FSI) simulation. The displacement of the internal nodes to a fluid mesh are derived from the given displacement of the structural nodes on the interface.

The interpolation function describing a displacement field for example is ap-

proximated by the sum of basis functions

$$S(\mathbf{x}) = \sum_{i=1}^{N_b} \alpha_i \phi\left(\|\mathbf{x} - \mathbf{x}_{b_i}\|\right) + p(\mathbf{x}) \tag{5.1}$$

where $\mathbf{x}_{b_i}$ are the coordinates with known displacement values, $p(\mathbf{x})$ is a polynomial and N_b the number of coordinates with known displacement. The function $\phi(d)$ is a basis function with respect to the euclidean distance d.

The minimal degree of polynomial $p(\mathbf{x})$ depends on the choice of basis function. Choosing to use conditionally positive definite basis functions of order $m \leq 2$ allows the use of a linear polynomial. This has the added advantage that rigid body translations are exactly recovered [26].

The coefficients α_i and polynomial are determined from interpolation conditions. This is done by solving the system

$$\begin{Bmatrix} \mathbf{d}_b \\ \mathbf{0} \end{Bmatrix} = \begin{bmatrix} \mathbf{M}_{b,b} & \mathbf{P}_b \\ \mathbf{P}_b^T & \mathbf{0} \end{bmatrix} \begin{Bmatrix} \boldsymbol{\alpha} \\ \boldsymbol{\beta} \end{Bmatrix} \tag{5.2}$$

with $\mathbf{d}_b$ the known displacements. $\mathbf{M}_{b,b}$ is an $n_b \times n_b$ matrix containing the evaluation of the basis function

$$\phi_{b_i b_j} = \phi\left(\left\|\mathbf{x}_{b_i} - \mathbf{x}_{b_j}\right\|\right). \tag{5.3}$$

$\mathbf{P}_b$ is an $n_b \times 4$ matrix with $\mathbf{P}_{b_i} = \begin{Bmatrix} 1 & x_{b_i} & y_{b_i} & z_{b_i} \end{Bmatrix}$. The coefficients α_i are contained in $\boldsymbol{\alpha}$ and $\boldsymbol{\beta}$ contains the coefficients of the linear polynomial. With the system solved, finding the displacement at an unprescribed coordinate in the field simply requires the evaluation of the interpolation function in Equation (5.1).

Various radial basis functions are available, many of them finding application within specific fields of research. In geometric morphology for instance, the thin plate spline (TPS) is commonly used to visualise modes of variation between subjects in a statistical sample or to visualise the difference between subjects [42, 54]. An example of one of these studies on the geometric morphology of African lowland Gorilla scapulae is illustrated in Figure 5.1. Here the landmarks are visible in (a) with the measurements in (b) and the transformed coordinates after applying the Procrustes[1] method in (c). The TPS radial basis function is finally used to illustrate

[1] Translation, reflection, orthogonal rotation and scaling of a set of points to best conform them to a set of reference points. The fit is evaluated using the sum of squared errors between corresponding points [42].

Name	Function
CP C^0	$(1-\xi)^2$
CP C^2	$(1-\xi)^4(4\xi+1)$
CTPS C^0	$(1-\xi)^5$
CTPS C^1	$1+\frac{80}{3}\xi^2-40\xi^3+15\xi^4-\frac{8}{3}\xi^5+20\xi^2 log(\xi)$
Linear	x
Cubic	x^3
Thin plate spline (TPS)	$x^2 log(x)$
Multi-quadratic bi-harmonic (MQB)	$\sqrt{a^2+x^2}$
Inverse multi-quadratic bi-harmonic (IMQB)	$(a^2+x^2)^{\frac{-1}{2}}$
Gaussian (G)	$exp(-x^2)$

Table 5.1: Some radial basis functions with compact support $f(\xi)$ and global support $f(x)$

the variation between male and female Gorilla scapulae.

Radial basis functions can be divided into two groups: functions with global support and functions with local support [26]. Local or compact support functions are generally scaled with a support radius r such that $\xi = x/r$. The basis function $\phi_r = \phi(\xi)$ is then used instead of the original $\phi(x)$.

Using compact support mainly moves the nodes within a circle or sphere of radius r around the nodes with known displacement. Large support radii result in greater support and so involves solving denser matrices. This is also always the case when dealing with functions with global support.

A list of RBFs are documented in Table 5.1. The MQB and IMQB methods have an additional parameter a that controls the shape of the function. Larger a values result in functions that are flatter with smaller values resulting in narrow cone-like functions.

Applying a few radial basis functions to the deformation of a base dolphin geometry is illustrated in Figure 5.2. For the two different dolphin geometries 14 landmark positions were marked manually. RBF interpolation is then used to deform the mesh if these points on the one dolphin is required to match the landmark positions on the target dolphin exactly.

Different functions have a totally different effect on the deformed mesh. From this simple example it seems that more landmarks are required to better deform the one geometry into an approximate representation of the other.

If a feature point registration procedure like shape context correspondence briefly

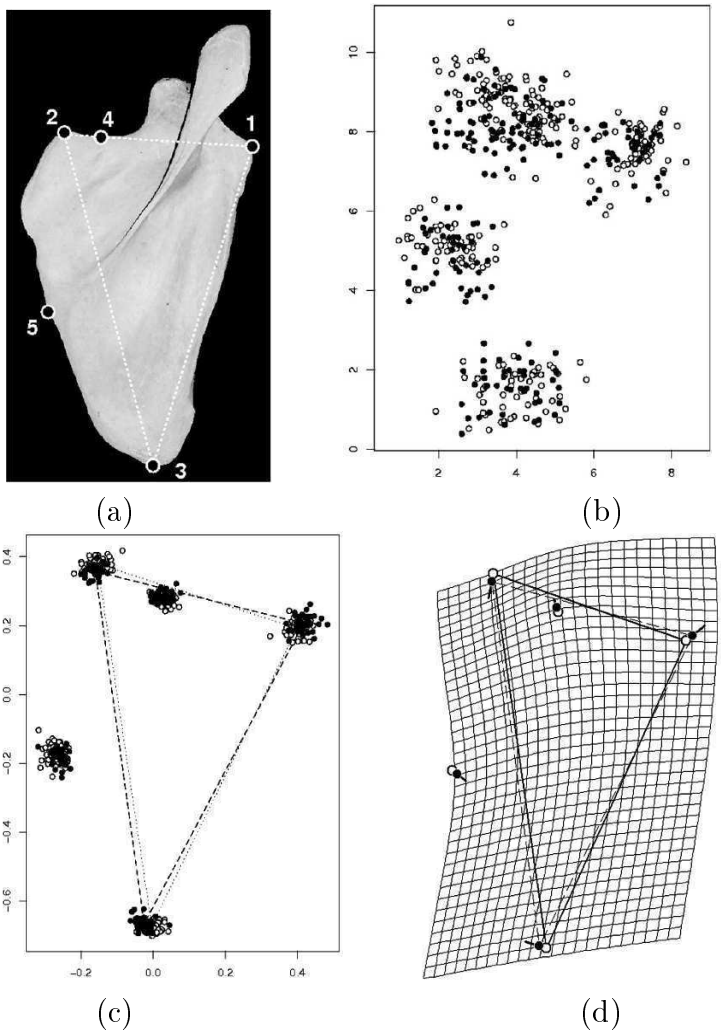

Figure 5.1: Geometric dissimilarity illustrating the average shape of the scapula of male ($n_m = 52$, *open symbols*) and female ($n_f = 42$, *closed symbols*) western African lowland Gorillas. (a) Recorded coordinates of homologous points on each specimen. (b) The varying coordinates due to difference in shape as well as location and orientation with respect to axes during landmark digitisation. (c) Superimposed landmark coordinates after applying the Procrustes method. The common coordinate system allows for further statistical analysis. (d) Visualising statistical results, the average male-female variation is shown using both difference vectors and a thin plate spline deformation grid magnified by a scale factor of two [54].

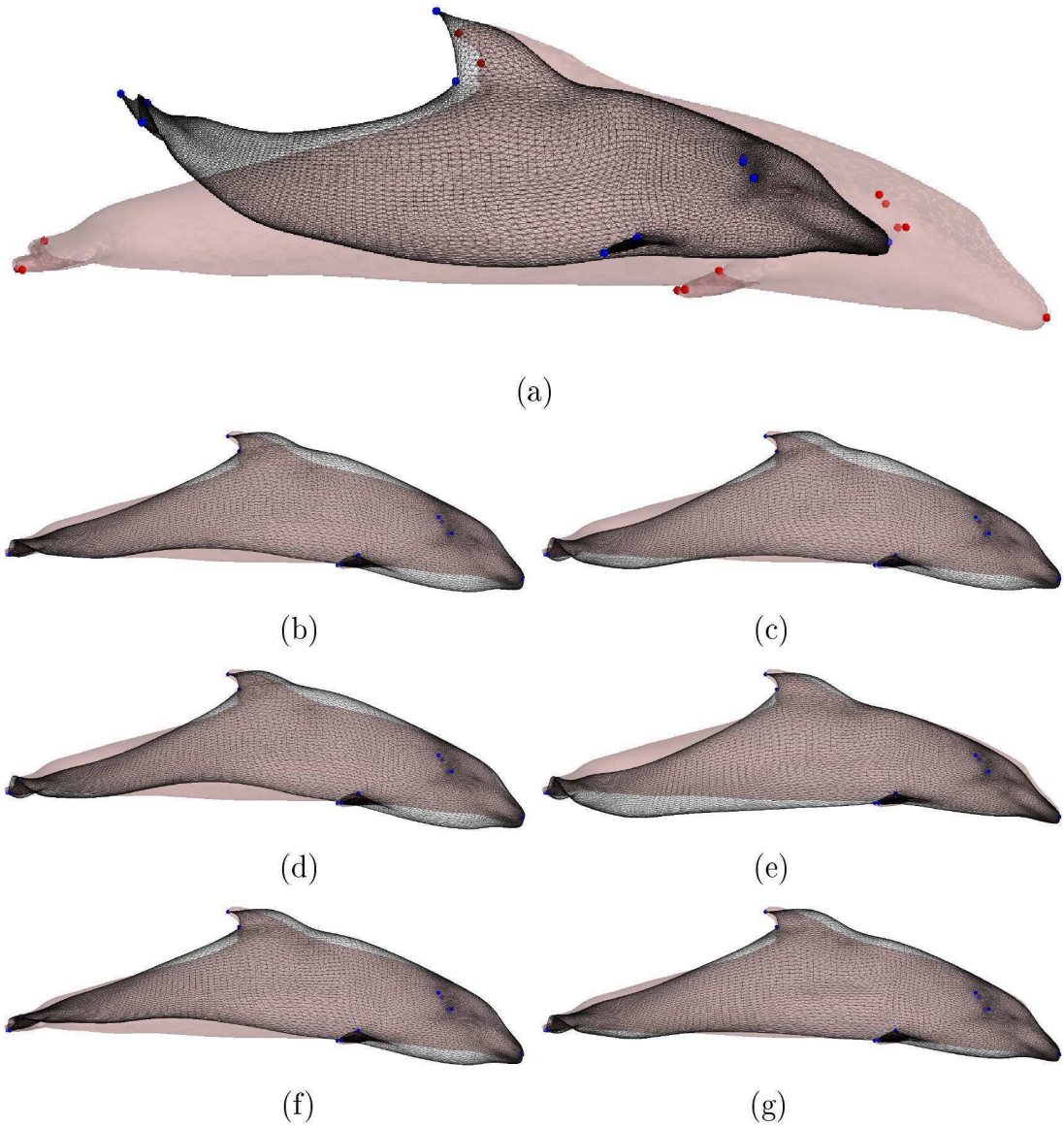

Figure 5.2: Radial Basis Function Performance. (a) Original Configuration (b) MQB, (c) IMQB, (d) Gauss, (e) Linear, (f) Cubic, (g) TPS. The deformable mesh is displayed as a black wire-frame and the target as the semi-opaque pink surface. The blue dots indicate deformable landmark positions and the red dots the target positions. In (b) through (g) these landmark coordinates coincide exactly.

discussed in Appendix C is used, deformation could be determined by radial basis function interpolation. It is decided that the scope of work covered by this report would not include additional surface registration procedures but only work with the original elastic surface registration procedure implemented. If landmark coordinates or landmark coordinate displacement is available, radial basis function interpolation could be used before performing full surface registration. This step would result in a preferred initial condition when performing elastic surface registration.

5.2 Feature Line Registration

Crest lines like those extracted from a surface mesh in subsection 4.3.4 of this report, or even those obtained from something like voxel density data, can be compared and registered. The methodology and approach of Subsol *et al.* [59] is explained in this section for matching sets of feature lines in a generic and target geometry.

In their work, correspondences are found between sets of features by using a non-rigid registration algorithm. Common features are identified and common feature subsets are used in creating an automatic anatomical atlas of the human skull. This is all done to finally average the features in the creation of the atlas from where a variability analysis is done on common feature positions. Their registration procedure is outlined in subsection 5.2.1 and the procedure implemented for this report is also detailed along with experimental results.

5.2.1 Registration Procedure

Given two sets of feature lines on two different geometries like that of Figure 5.3, the aim of Subsol *et al.* is to match and extract common features. A twofold result is sought [59] :

- Line correspondence: which line L_i on the target geometry $\mathcal{P}$ corresponds to a line L_j of geometry $\mathcal{M}$. This allows extracting the common lines to all models in the statistical set used in creating the atlas.
- Point correspondence: the points of each skull that correspond to the points on the skulls over the different sets are required. This is needed to finally do the averaging of the lines and also study inter-patient variability.

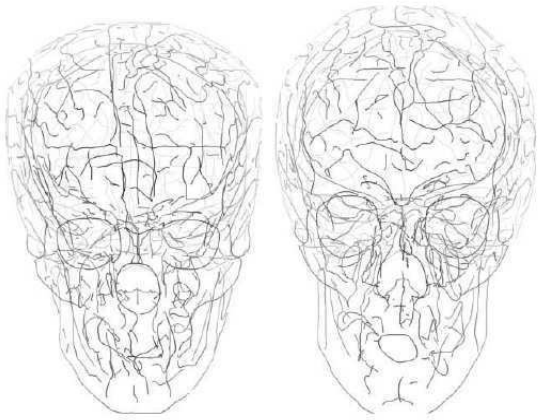

(a) (b)

Figure 5.3: Two sets of lines to be registered [59]. (a) The target skull $\mathcal{P}$ on the left is composed of 591 lines and 19'302 points. (b) Reference skull $\mathcal{M}$ on the right is composed of 583 lines and 19'368 points. These subjects have a variation in shape as well as differences in the number and topology of the lines.

The registration procedure proposed in their work uses a heuristic algorithm based on an iterative scheme, gradually updating the local registration. In implementing this, each feature location influences matching decisions made at other locations. This is done as an adaptation of the ICP [13] where the deformations between anatomical structures are modelled by affine, polynomial and spline functions.

Point Matching

At each iteration the points of the lines of $\mathcal{M}$ are linked with their closest neighbour in the lines of $\mathcal{P}$ with respect to the Euclidean distance. This preliminary simple matching gives an initial list of point pairs. From Figure 5.4, it is seen that this simple closest point match is not bijective[2]. Here each point on the reference geometry feature set only has a single match whereas points on the target could have no correspondent or even more than one.

[2] A bijective match means that two conditions are satisfied: (1) Every one point in the model point set $\mathcal{M}$ is registered to at most one point in the data point set $\mathcal{P}$ (Injective / one-to-one). (2) Every point in the data point set $\mathcal{P}$ has at least one point match on the model set $\mathcal{M}$ (surjective / onto).

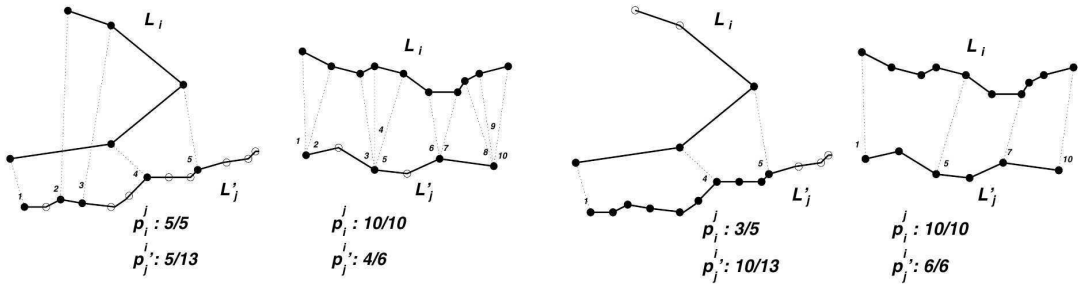

(a) (b)

Figure 5.4: Registering two lines [59]. (a) Illustration revealing that computing registration parameters is not obvious due to the non-bijectivity of matched points. (b) After discarding non-consistent matched points, line registration parameters are computed consistently.

Line Matching

In estimating whether two lines $L_i \in \mathcal{M}$ and $L'_j \in \mathcal{P}$ are registered, the portion of points of one line registered to the points of another line is needed.

The portion p_i^j of points on line L_i registered to L'_j and the portion p'^i_j of points on line L'_j registered to L_i are used. If p_i^j or p'^i_j is larger than a given threshold, it can be seen as a positive registration. Due to the non-bijectivity of the matched points, computing these registered portions is not simply done with the initial closest point registrations.

In Figure 5.4, this non-bijectivity is visible. In the example of a registration obtained in Figure 5.4 (a), 100% of line L_i is registered to 40% of L'_j. The points at 2 and 3 are joined to a portion of L_i that is invalid. This causes a cross match, resulting in non-physical deformation. In the example of a registration in Figure 5.4 (a), the multiple matching scenario is visible. These problems are addressed by introducing two additional constraints:

- An injectivity[3] constraint allows at most one link made between a point on L'_j and a point on L_i.
- The ordering of corresponding points are checked. This implies that the same portion of L'_j can not be matched to different portions of L_i.

[3] A one-to-one match for at least each point in the model shape $\mathcal{M}$ is injective. Every point in the model point set is registered to at most one point in the data point set $\mathcal{P}$

The additional constraints are imposed by sorting the matched points according to their distance. This is because closer corresponding pairs are more likely to be a correct match. The most likely matched point p_0 of L_i is chosen as a starting point. The line is then followed in both directions. Each correspondence along a direction is inspected and treated accordingly:

- If the correspondence is made to a point on another line than that of p_0, the search propagation along that direction of the line is discontinued.
- If the corresponding point has already been marked, a cross or multiple matching could be present and the current matching is discarded. Further propagation along that direction of the line is again discontinued.
- If the correspondence has not been marked, the matching is kept. All points between the previous and the current matched point on L'_j are marked as also being matched to the line segment connecting the two matched points on L_i.
- Once the process has terminated, it is repeated using the next most likely match.

Treating initial matched points in this way, Subsol *et al.* [59] obtain a consistent point correspondence. Although points marked between positive matched points on the same line segment of L'_j aren't explicitly matched, their matches are used in determining the matched point portions p_i^j and p'^i_j. This procedure does not suddenly make the match bijective but at least allows for a consistent mapping from $\mathcal{M}$ to $\mathcal{P}$. Multiple matches onto the same point and cross matches are removed.

Registration portions are checked when applying the registration. Only the registration to lines above a user specified registration threshold is applied. If a threshold of 50% is chosen for example p_i^j, p'^i_j or both need to be above the required threshold for it to qualify as a positive registration.

Transformation Computation

Based on the matched points, Subsol *et al.* [59] compute a transformation T by minimising the least squares criterion:

$$\sum_{k \in \mathcal{M}^j} \left\| T\left(p_k^j\right) - p'^k_j \right\|_2^2 . \tag{5.4}$$

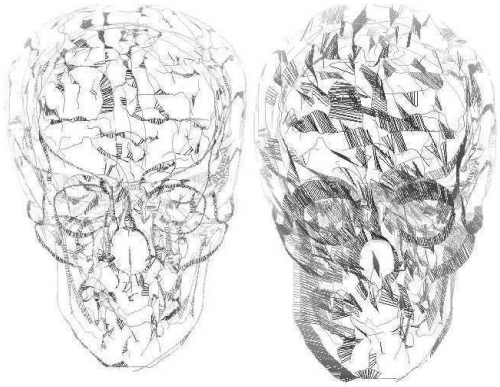

(a) (b)

Figure 5.5: Registration of $\mathcal{M}$ towards $\mathcal{P}$ [59]. (a) The deformed set $\mathcal{M}$ with $\mathcal{P}$. Matched points are linked with the two sets reasonably superimposed. In (b) $\mathcal{M}$ is in it's original position, allowing an estimated extent of the deformation between the two sets.

Here k resembles a matched point out of the total point correspondence list $\mathcal{M}^j$. This point of $\mathcal{M}$ and it's corresponding point in $\mathcal{P}$ are given as p_k^j and p'^k_j.

In their procedure Subsol *et al.* [59] used a constant iteration scheme. 30 iterations are performed with the required registration threshold incremented from 0% to 50%. In the first 10 iterations rigid transformation is applied. 10 iterations of affine transformation[4] is followed and the final 10 iterations are used to apply spline transformations.

The registration of one skull's feature lines to another in Figure 5.3 as done by Subsol *et al.* is seen in Figure 5.5. To build the anatomical atlas, six skulls were registered to one another and the registration used in setting up a registration map. This registration map is used as a consistency check and an example of one of these maps is displayed in Figure 5.6.

The registration map is used to extract features common to all subjects in the sample. These common features and their positive registrations are used to build the final skull atlas shown in Figure 5.7.

[4]An affine transformation between two vector spaces comprises a linear transformation and translation. Mapping $\mathbf{x}$ to a different vector space with an affine transformation: $\mathbf{x} \mapsto \mathbf{A}\mathbf{x} + \mathbf{b}$.

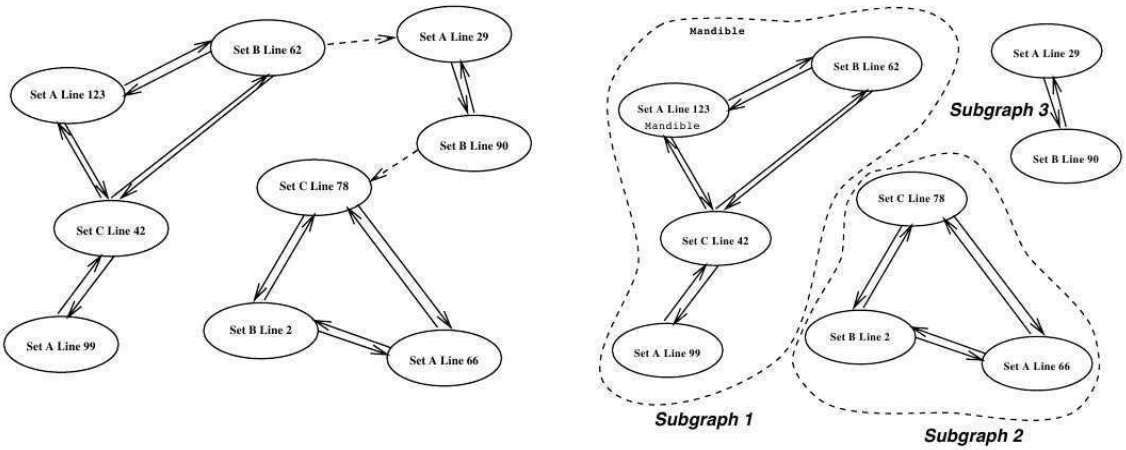

(a) (b)

Figure 5.6: Building and using a topological registration map [59]. (a) The registration graph: each node is a line of a set and an oriented link represents the relation "is registered with". (b) Extracted subsets of corresponding lines of different data sets. If a sub-graph contains at least one line of each data set, it defines a subset of common lines found on all geometries in the sample.

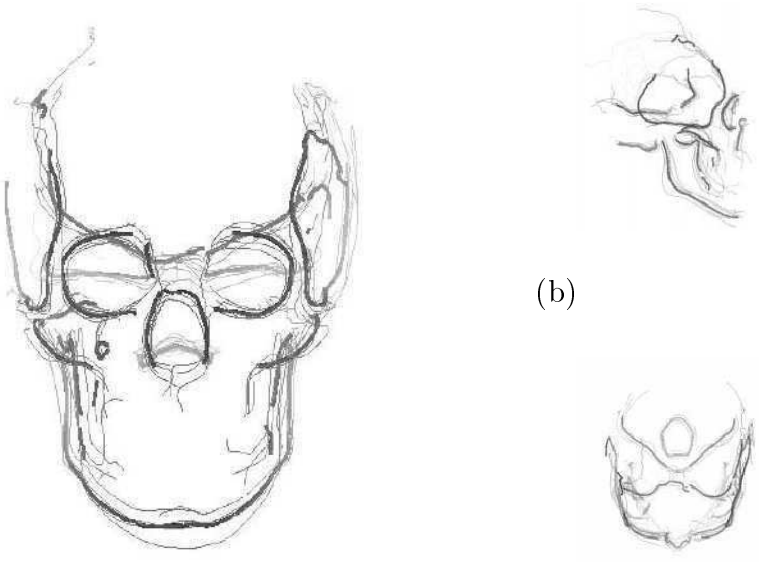

(a) (b) (c)

Figure 5.7: Common lines to all six skulls used by Subsol *et al.* [59]. The thin lines show the lines of the different geometries used and the thicker lines the average common lines constituting the atlas.

Implementation

In this report a slightly different procedure was implemented. The same ideas presented in [59] are used but combined with work done on the full surface registration implemented earlier in this study. After obtaining the feature lines:

- The target object $\mathcal{P}$ is first oriented to best fit the generic shape $\mathcal{M}$ using the iterative closest point procedure described in subsection 3.1.1.
- Point correspondences are obtained in the same way as done by Subsol *et al.* [59]. This is however not only done for $\mathcal{M}$ onto $\mathcal{P}$ but also for $\mathcal{P}$ onto $\mathcal{M}$. An additional requirement is also added that the dot product of matched point unit normals be greater than zero.
- Correspondences with a distance greater than a user specified value is discarded.
- Correspondences are filtered for both sets in the same way as Subsol *et al.* [59] to get rid of inconsistent point matches.
- The closest line segment to each inexact matched point is inspected. The closest point on that line segment is determined as a possible final matched coordinate.
- Using the matched points and their registered positions, a smooth deformation field is applied. This is done as in the elastic surface registration algorithm of Bryan *et al.* [19] with the use of Equation (3.8).
- Registration and deformation is applied iteratively using the same parameters as in the original elastic registration procedure of subsection 3.2.1.

Application

The performance of the implemented feature registration procedure is illustrated using two dolphin geometries. The two original geometries is obtained from the INRIA model shape repository [4]. The one geometry is then refined, manipulated and smoothed to generate the target geometry in the feature registration example. The other geometry is only refined and smoothed. Registration of the features on the dolphin geometries is presented in Appendix D of this report with only the lateral views of Figures D.1 through D.3 reproduced in Figure 5.8 for visual clarity.

Crest lines on the two geometries are extracted and thresholded to get rid of less significant lines. The target geometry and it's crest lines are displayed in Figure 5.8 (a) and D.1. In this figure the lines on the generic dolphin shape is also displayed in it's original position.

A rigid registration is performed on the target geometry allowing isotropic scale with upper and lower constraints set as 0.5 and 1.5. The results of the isotropic scale ICP registration is displayed in Figures 5.8 (b) and D.2. After rigid registration, the feature line registration procedure is implemented to deform the lines on the generic dolphin geometry to better represent that of the target. Registered and deformed lines are visible in Figures 5.8 (c) and D.3. Only registered lines with a matched point portion of at least 50% are used and displayed.

5.3 Surface registration

Creating a symmetric smoothed skull with elastic surface registration is again performed. The smooth skull and it's reflection is taken in their position relative to one another following the rigid registration procedure discussed in section 3.3.

Registration of the ridge and valley lines of the skull onto the lines of its mirrored projection is performed before the elastic registration procedure. Lines on the smooth skull and it's reflection are visible in Figures 5.9 and 5.10. These figures demonstrate the registration of the one set of lines onto the other. After feature registration the average nodal coordinates before and after is obtained and also displayed. These average feature lines are noticeably more symmetric than the lines on the original smoothed skull geometry.

The deformed skull after feature registration is used as the initialised deformable surface when performing the elastic registration procedure. The final registration and the averaged symmetric skull representation are visible in Figures 5.11 (c) and (d).

To view the asymmetry of the original skull shape, the displacements back to the original skull form is used and applied with a factor of three. This asymmetry is displayed in Figure 5.12 (a). The distance from the averaged symmetric shape to the equivalent nodal coordinate on the original surface is also displayed in Figure 5.12 (b). In Figure 5.12 (b) the non-uniqueness of the registration procedure as inspected in subsection 3.2.2 is again visible. This is noticed when considering that the absolute distance value from the original mesh nodes to the symmetric

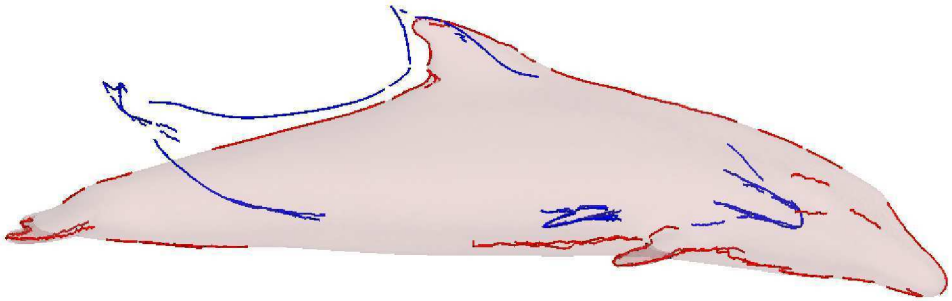

(a)

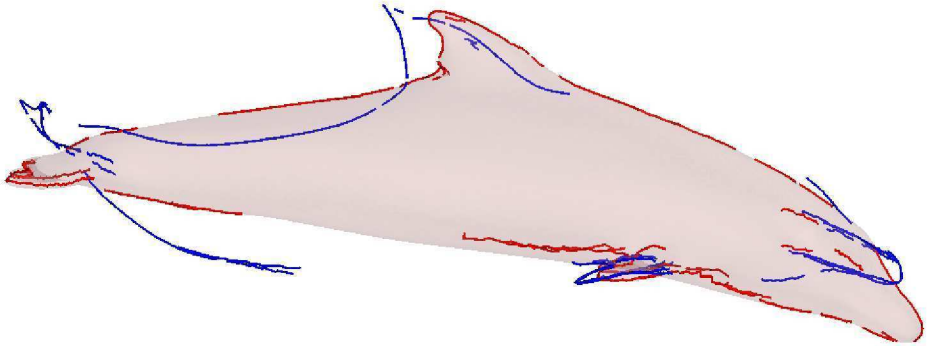

(b)

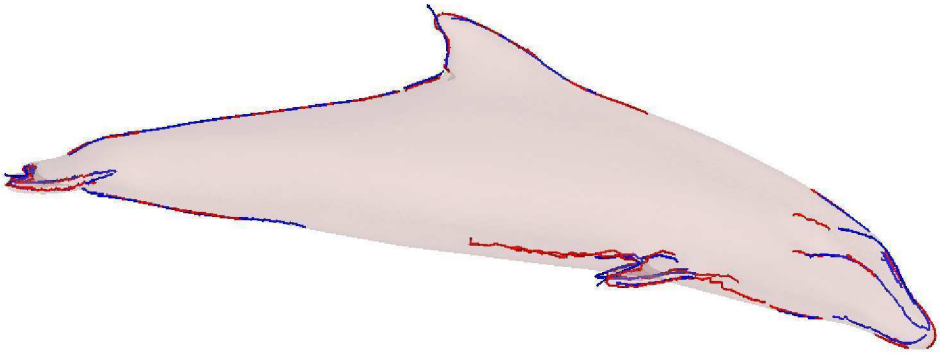

(c)

Figure 5.8: Feature line registration on dolphin geometries. (a) Original position of a target and base dolphin geometry. (b) Updated position of the target dolphin geometry relative to the base shape after isotropic scale ICP registration. (c) Feature registration of the base dolphin to the aligned target configuration at iteration 100. The target geometry is illustrated in its aligned position with the target features in red and the deformed base geometry features in blue.

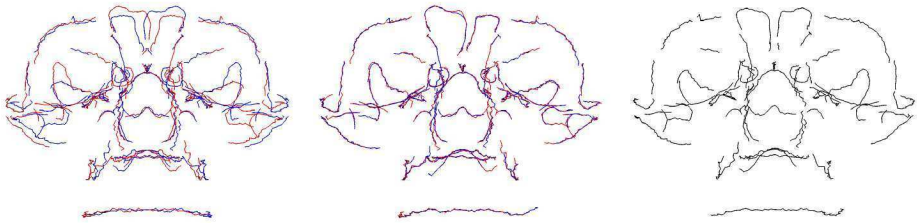

(a) (b) (c)

Figure 5.9: Frontal view of feature registration on the smooth skull and its reflection. (a) Feature lines of the smoothed skull and its reflection. (b) Feature registration result and (c) the average of the initial and registered positions to create a symmetric model. Blue lines indicate the features of the deformable surface with red lines indicating the target features.

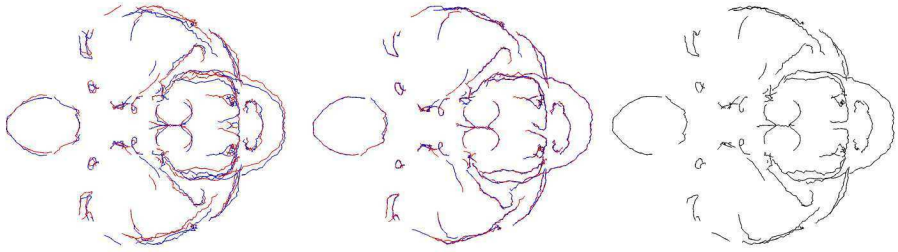

(a) (b) (c)

Figure 5.10: Lower view of feature registration on the smooth skull and its reflection. (a) Feature lines of the smoothed skull and its reflection. (b) Feature registration result and (c) the average of the initial and registered positions to create a symmetric model. Blue lines indicate the features of the deformable surface with red lines indicating the target features.

version is not in itself symmetric. It would seem that one side of the skull mesh has to deform more than the other side in order for a symmetric version to appear. The overall appearance of the color contours in Figure 5.12 (b) however is mainly symmetric in the facial region.

The results obtained in this chapter is compared to the initial registration results of Figure 3.11. Comparing these results in Figure 5.13, there is an improvement in the registered generic mesh when first applying feature registration.

5.3.1 Orthognathic Representation

The symmetric version of the smoothed skull is done to create an example generic skull surface for use in subsequent registrations. To test the registration of this

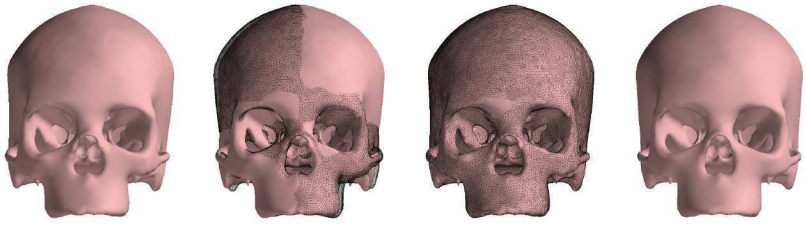

(a) (b) (c) (d)

Figure 5.11: Elastic surface registration of the smooth skull onto its reflection. The blue mesh in Figure 3.10 is set as the deformable mesh and is registered onto it's reflection. (a) Reflected smooth skull geometry. (b) Reflected smooth skull geometry set as the target with the original smooth skull shown as the black wire-frame. (c) Elastic surface registration results after first applying the feature registration of Figures 5.9 and 5.10. (d) The average of the smooth skull and registered nodal coordinates resulting in a symmetric skull surface.

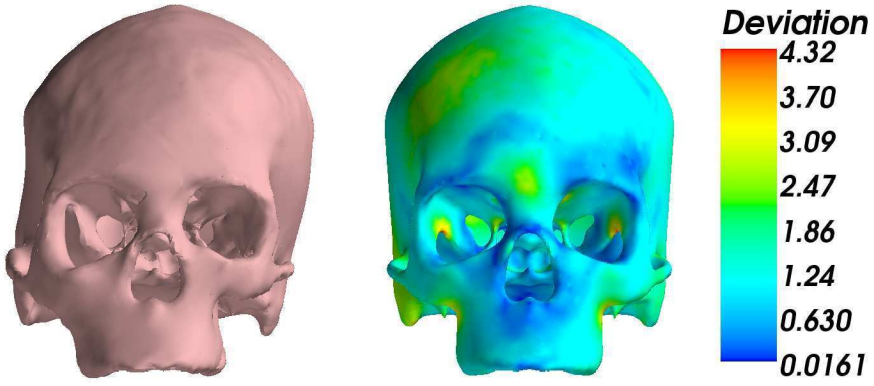

(a) (b)

Figure 5.12: Asymmetry in the original smooth skull geometry. (a) Displacement from the symmetric skull mesh coordinates back to the original scaled by a factor of 3. (b) The absolute distance (norm of the distance vector) from the original to symmetric nodal coordinates illustrated as scalars on the symmetric skull representation. The color bar values are in millimeters.

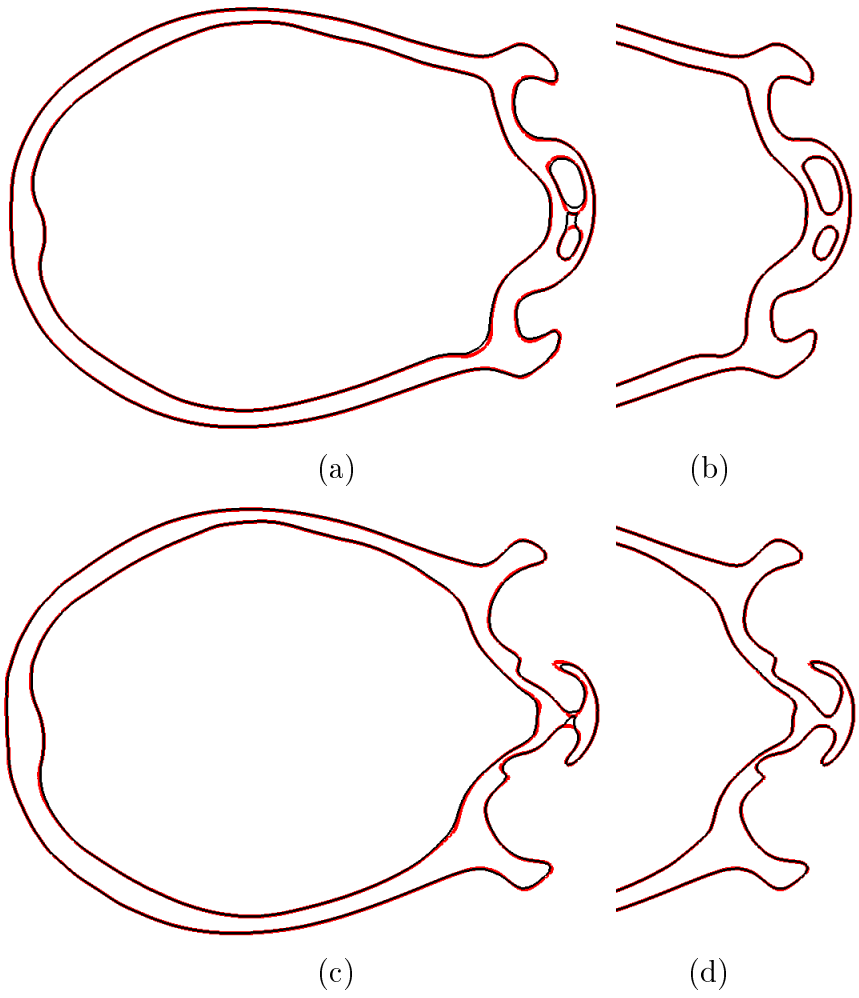

Figure 5.13: Reflected registration incorporating an initial feature match. Simply registering the smooth skull geometry onto it's reflection in Chapter 3 created problems with especially the sinuses. The same cut planes of Figure 3.11 are presented here compared to the registration result after an initial feature match. (a), (c) The initial registration and (b), (d) result after initial feature registration at iteration 100. Recall that the red line indicates the target geometry in the plane with black the surface deformed during registration.

generic shape to a new skull geometry elastic surface registration is performed on the original orthognathic skull.

After a rigid registration, the orthognathic skull is aligned to the generic shape and the generic shape is deformed to represent the target. The registration of the generic shape to the orthognathic skull is done by first performing a feature registration and then a surface fitting. Feature lines on the generic shape and orthognathic surface are registered and the deformed generic surface is used as an input to the elastic surface registration procedure. The resultant registration and deformed generic shape is visible in Figure 5.14.

From the registration results visible in Figures 5.14 through 5.17, a full registration seems undesirable. Unmatched features are not used in the feature registration but the surfaces associated with these still affect the elastic surface registration. For this reason it would be beneficial to describe a registration to unmatched feature areas of the target and generic surface as unallowable.

The effect of unmatched features on the registration could be automatically reduced by restricting registration to areas of the surface mesh associated with these unmatched features. Registration restriction is explained and implemented in the proposed combination of procedures, presented in the next chapter. This reduces the amount of user interference required in adequately deforming the generic shape into a representation of the orthognathic skull form for example.

In Figure 5.17 significant deformation is seen to occur in the noisy internal areas during smoothing, indicating that the problem has reached the final stage. An example of what happens at this stage is visible on the femur problem convergence plots in Figure 3.7. In the smoothing stages of the procedure, the smoothing done to improve element quality removes the inconsistent localised deformation and high frequency surface noise applied during registration. This manifests as peaks in the convergence plots.

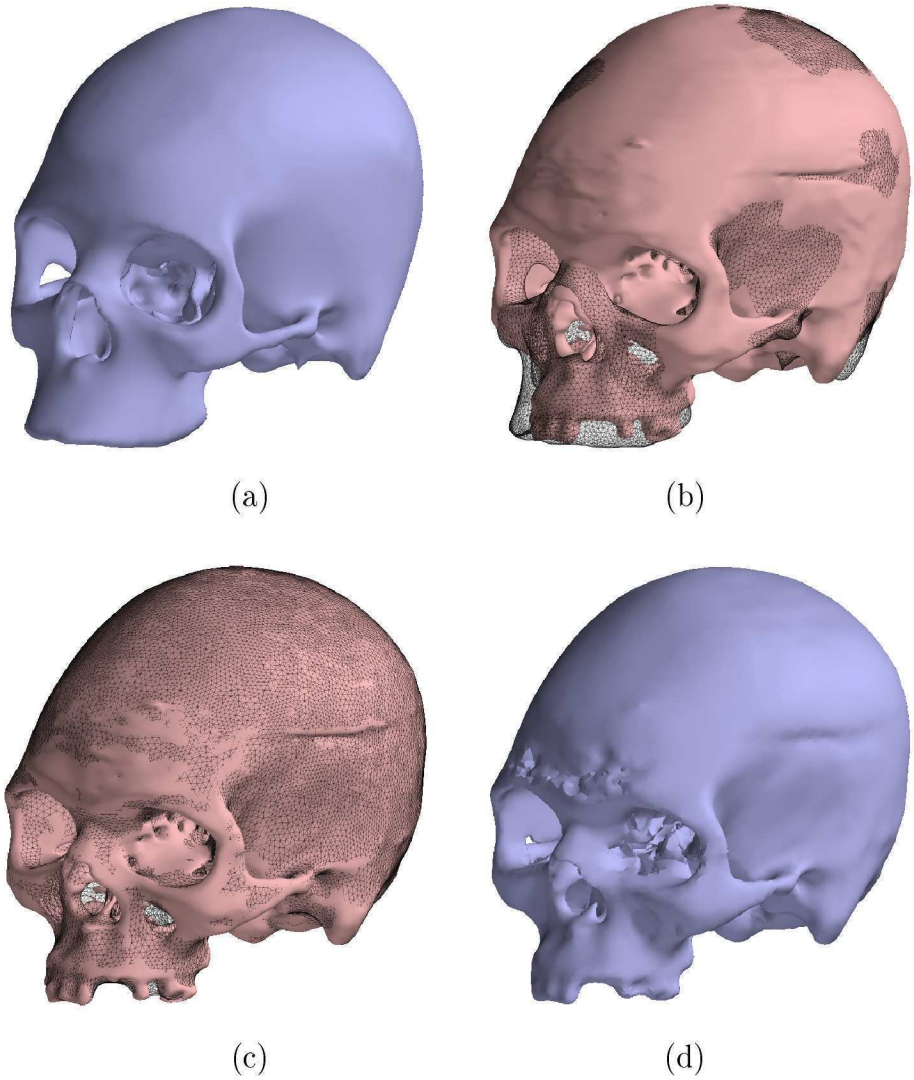

Figure 5.14: Elastic registration on the orthognathic skull. (a) The initial deformable mesh. (b) The rigid registration result to align the orthognathic skull to the deformable mesh with (c) the registration result at iteration 60. (d) The smoothed deformed mesh at iteration 60.

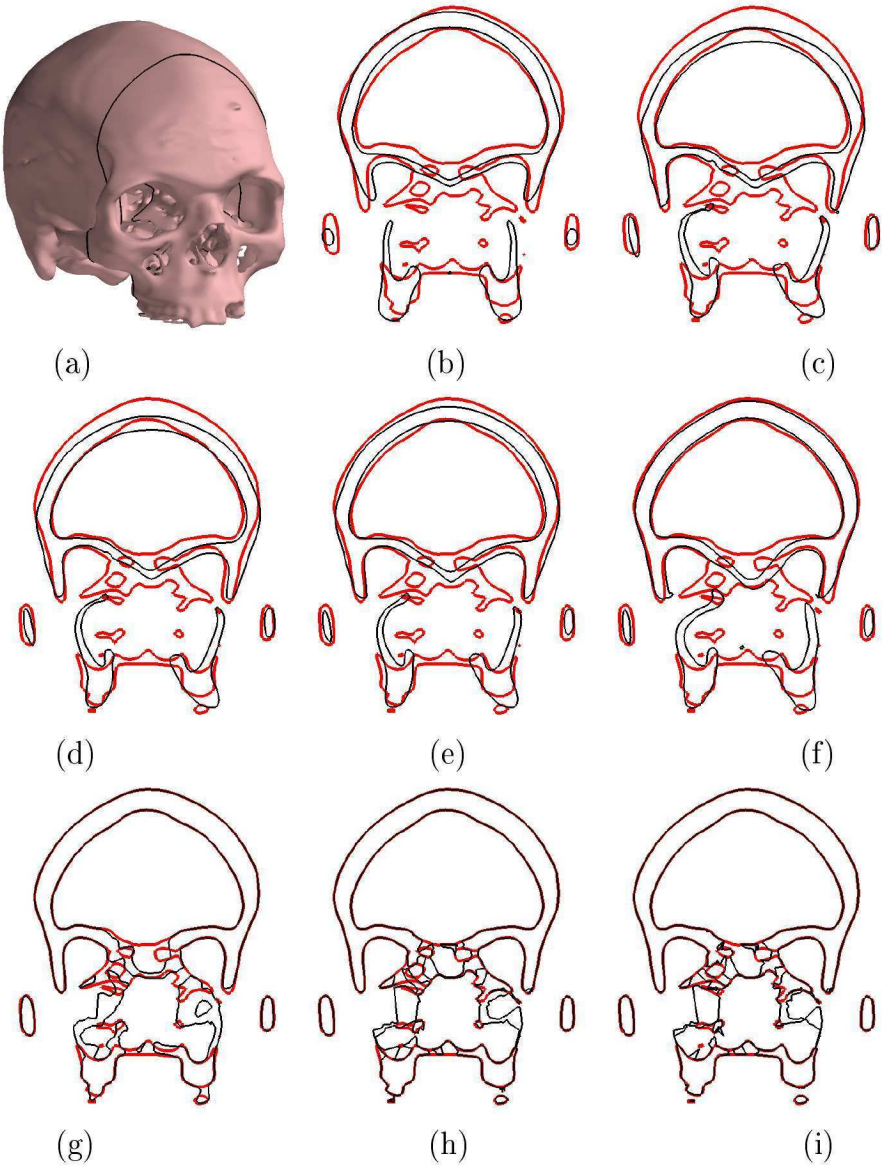

Figure 5.15: Frontal view of elastic registration on the orthognathic skull. (a) The cut plane illustrating the position of the subsequent figures taken for the registration result. (b) The target and deformable geometry after isotropic scale ICP registration. (c) The result of an initial surface feature registration. Elastic surface registration is performed after an initial feature registration resulting in base mesh deformation at iteration (d) 10, (e) 20, (f) 30, (g) 40, (h) 50 and (i) 60. The red line represents the position of the target surface in that plane and the black line the deformable mesh surface. Note that the topology doesn't change although it might appear that way. This appearance is due to the registered feature coming in and out of the plane where these figures are generated.

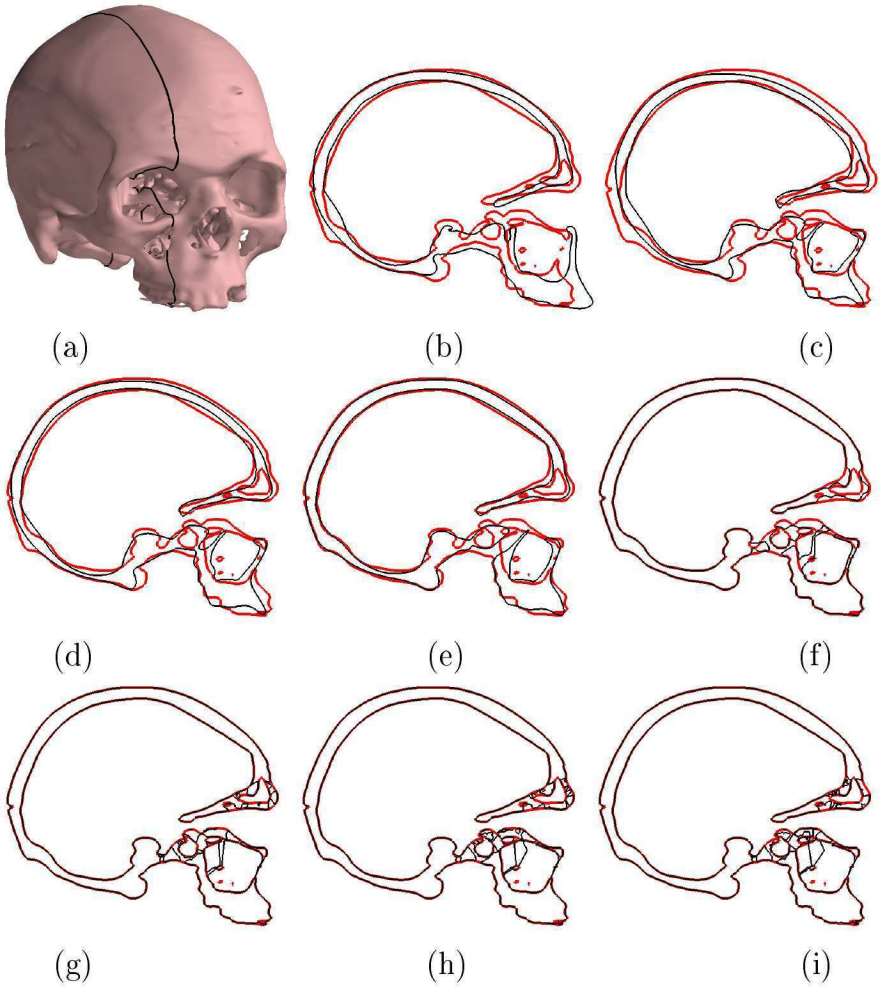

Figure 5.16: Lateral view of elastic registration on the orthognathic skull. (a) The cut plane illustrating the position of the subsequent figures taken for the registration result. (b) The target and deformable geometry after isotropic scale ICP registration. (c) The result of an initial surface feature registration. Elastic surface registration is performed after an initial feature registration resulting in base mesh deformation at iteration (d) 10, (e) 20, (f) 30, (g) 40, (h) 50 and (i) 60. The red line represents the position of the target surface in that plane and the black line the deformable mesh surface.

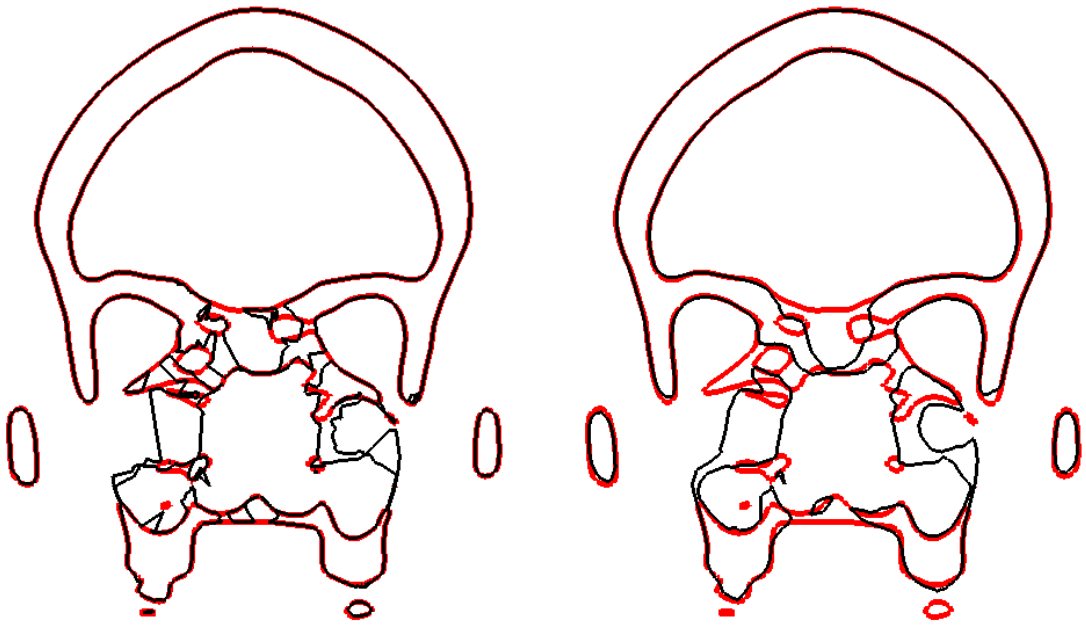

(a) (b)

Figure 5.17: Difference between the original and smoothed registration result at iteration 60. (a) Result of the elastic surface registration at iteration 60. This is the same cut as visible in Figure 5.15 (i). (b) The result showed in (a) after 10 Taubin [61] smoothing iterations. The red line represents the position of the target surface in the cut plane and the black line the deformable mesh surface.